

Journal of Photonics for Energy

SPIEDigitalLibrary.org/jpe

Highly efficient blue organic light-emitting diodes using dual emissive layers with host-dopant system

Bo Mi Lee
Hyeong Hwa Yu
You Hyun Kim
Nam Ho Kim
Ju An Yoon
Woo Young Kim
Peter Mascher

Highly efficient blue organic light-emitting diodes using dual emissive layers with host-dopant system

Bo Mi Lee,^a Hyeong Hwa Yu,^a You Hyun Kim,^b Nam Ho Kim,^b
Ju An Yoon,^b Woo Young Kim,^{a,b} and Peter Mascher^a

^aMcMaster University, Department of Engineering Physics and Centre for Emerging Device Technologies, Hamilton, Ontario L8S 4L7, Canada

mascher@mcmaster.ca

^bHoseo University, Department of Green Energy and Semiconductor Engineering, Asan, 336-795, Republic of Korea

Abstract. We fabricated highly efficient blue organic light-emitting diodes (OLEDs) by designing differing emitting layer structures with fluorescent host and dopant materials of 4,4-bis (2,2-diphenylvinyl)-1,10-biphenyl and 9,10-bis (2-naphthyl) anthracene as host materials and 4,4'-bis (9-ethyl-3-carbazovinyleno)-1,1'-biphenyl (BCzVBi) as a dopant material to demonstrate electrical and optical improvements. Best enhancement in luminance and luminous efficiency were achieved by a quantum well structure in device F with 8668 cd/m² at 8 V and 5.16 cd/A at 103.20 mA/cm², respectively. Among the blue OLED devices doped by BCzVBi, device B emits the deepest blue emission with Commission Internationale de l'Éclairage coordinates of (0.157, 0.117) at 8 V. © The Authors. Published by SPIE under a Creative Commons Attribution 3.0 Unported License. Distribution or reproduction of this work in whole or in part requires full attribution of the original publication, including its DOI. [DOI: [10.1117/1.JPE.3.033598](https://doi.org/10.1117/1.JPE.3.033598)]

Keywords: dual emissive layer; luminous efficiency; blue OLED; quantum well; host-dopant; 4,4-bis (2,2-diphenylvinyl)-1,10-biphenyl; 4,4'-bis (9-ethyl-3-carbazovinyleno)-1,1'-biphenyl; 9,10-bis (2-naphthyl) anthracene.

Paper 12066P received Dec. 13, 2012; revised manuscript received Feb. 20, 2013; accepted for publication Mar. 8, 2013; published online Apr. 9, 2013.

1 Introduction

Organic light-emitting diodes (OLEDs) have attracted considerable interests due to their potential uses, such as full-color displays and solid-state lighting,¹⁻³ when Tang and Van Slyke⁴ reported the first multilayered OLEDs. Since then, much research has been conducted to improve OLED performance in terms of efficiency, color stability, and lifetime.⁵ Specifically to be commercialized, high-quality RGB primary colors are required and blue emission is necessary to achieve reliable white emission and full-color realization. A lot of effort has been exerted toward researching blue-emitting materials and improving color purity, as well as the efficiency, of blue OLEDs, because their performances still lag behind red- and green-emitting materials and devices.⁶⁻⁸ Major challenges for blue emission correspond to the wide energy band gap of dopants and matching host materials to achieve blue color, appropriate alignment between blocking layers and wide gap layers, and high energy exciton confinement.⁹ In recent years, it has been accepted that developing deep blue electroluminescence (EL) color with a Commission Internationale de l'Éclairage (CIE_xy) 'y' value of <0.15 is essential.⁵ Even though it is reported that some blue OLEDs emit a pleasing deep blue color, still efficiency remains an issue that should be improved in order to obtain lower power consumption.

The fluorescent OLED's efficiency is usually lower than a phosphorescent OLED, making it a challenge to improve its efficiency to the level of phosphorescent OLEDs. It is widely known that a host-dopant system can greatly improve device performance in terms of EL luminous efficiency and color stability.¹⁰ Therefore, better matching between the host material and deep blue dopant material with sufficient spectral overlap for Förster energy transfer¹¹ is required for deep blue emission with high efficiency.¹²⁻²⁰ Also, an OLED's quantum efficiency is determined

by the carrier injection and recombination in the emitting layer (EML); therefore, the balance between electrons and holes in the EML is the most important factor to obtain higher quantum efficiency.

This study contributes to the understanding of significant effects of double EMLs and host-dopant systems of blue OLEDs with 4,4'-bis (9-ethyl-3-carbazovinylylene)-1,1'-biphenyl (BCzVBi) doped to two different host materials of 4,4-bis (2,2-diphenylvinyl)-1,10-biphenyl (DPVBi) and 9,10-bis (2-naphthyl) anthracene (ADN). Variable combinations of host and dopant in single and dual EMLs were observed in blue OLED devices and their electrical and optical characteristics were compared to each other to achieve best luminous efficiency and blue color coordinates.

2 Experiment

Indium tin oxide (ITO) coated glass was cleaned in an ultrasonic bath in the order of acetone, methanol, diluted water, and isopropyl alcohol. Then the cleaned ITO was treated by O₂ plasma under the conditions of 2×10^{-2} Torr, 125 W for 2 min,²¹ and organic and metal layers of blue OLEDs were fabricated using a high vacuum (1.0×10^{-7} Torr) thermal evaporation.

The standard device structure used in this study is as follows: ITO/N,N'-diphenyl-N,N'-bis (1-naphthyl)-1,1'-biphenyl-4,4'-diamine (NPB) as a hole-transport layer (HTL) (700 Å)/EML (300 Å)/4,7-diphenyl-1,10-phenanthroline (BPhen) as an electron transport layer (ETL) (300 Å)/lithium quinolate (Liq) as an electron injection layer (20 Å)/aluminum (1000 Å). Figure 1(a) shows the molecular structures of the organic materials used in the blue OLED devices in which the EMLs are composed of DPVBi, and, and BCzVBi, and Fig. 1(b) shows the schematic diagram of the blue OLED configuration. Six devices with different EML structures are shown in Table 1 and are classified by different host materials, the sequence of host materials, and doped or nondoped EMLs. The EML thickness is fixed at 300 Å regardless of the EML structures.

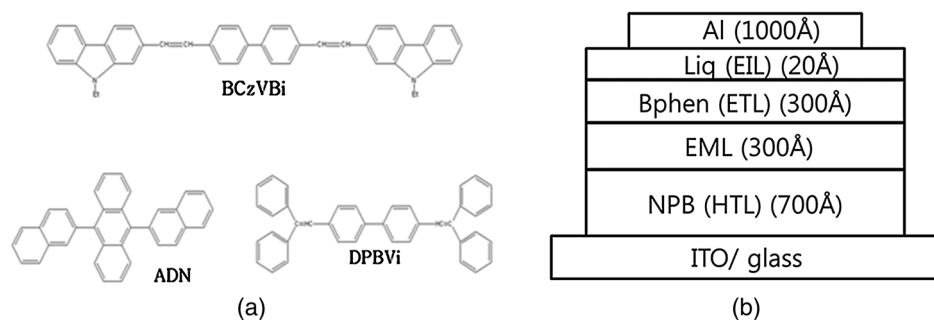


Fig. 1 (a) Fluorescent host and dopant materials for blue emission, and (b) the standard structure of blue OLED devices.

Table 1 EML composition of blue OLED devices A to F.

	EML structure
Device A	DPVBi (300 Å)
Device B	ADN (300 Å)
Device C	DPVBi (150 Å)/ADN (150 Å)
Device D	ADN (150 Å)/DPVBi (150 Å)
Device E	DPVBi:BCzVBi (15%) (300 Å)
Device F	DPVBi:BCzVBi (15%) (150 Å)/ADN:BCzVBi (15%) (150 Å)

With various DC voltage biases, the optical and electrical properties of blue OLEDs, such as the current density, luminance, luminous efficiency, CIE_{xy} coordinates, and EL characteristics, were measured with a Keithley 236, CHROMA METER CS100A and IVL-200 (JBS International, Korea) OLED analysis system.

3 Results and Discussion

ADN and DPVBi are used as the fluorescent blue emitter in the devices in this paper. As shown in Fig. 2(a), the current densities of devices A to D are 142.8, 161.2, 141.2, and 189.3 mA/cm² at a bias of 8 V, respectively. Typically, the current density is determined by the charge carrier injection from carrier transport layers²² and the injection is affected by the highest occupied molecular orbital (HOMO) to the lowest unoccupied molecular orbital (LUMO) energy level configuration of organic materials in the devices.

In spite of the 0.2 eV higher LUMO energy levels between ADN and BPhen, the higher current density is achieved in device B with a highly applied voltage because the electron mobility of ADN is one order of magnitude higher than its hole mobility.²³ Devices A and C show similar curves with variable applied voltage and relatively lower current density, while device D has the highest current density due to the structural advantage in the energy band diagram, as shown in Fig. 3. The LUMO of DPVBi is 0.2 eV lower than the LUMO of ADN. These HOMO-LUMO energy levels in organic layers can explain that device D has a stepped structure with a lower energy offset between adjacent layers as compared to other devices. This well-arranged structure leads to more effective electron transport and higher current density than other devices. In devices A and C, the large energy offset of 0.7 eV between DPVBi and NPB plays a role in blocking electrons and it consequently leads to the lowest current density.

The plots of luminance versus voltage and luminous efficiency versus current density of devices A to D are shown in Fig. 2(b) and 2(c). Device A has the highest luminance and luminous efficiency of 3708 cd/m² at 8 V and 2.81 cd/A at 99.86 mA/cm², and device C shows second highest luminance of 2946 cd/m² at 8 V and 2.21 cd/A at 102.88 mA/cm²,

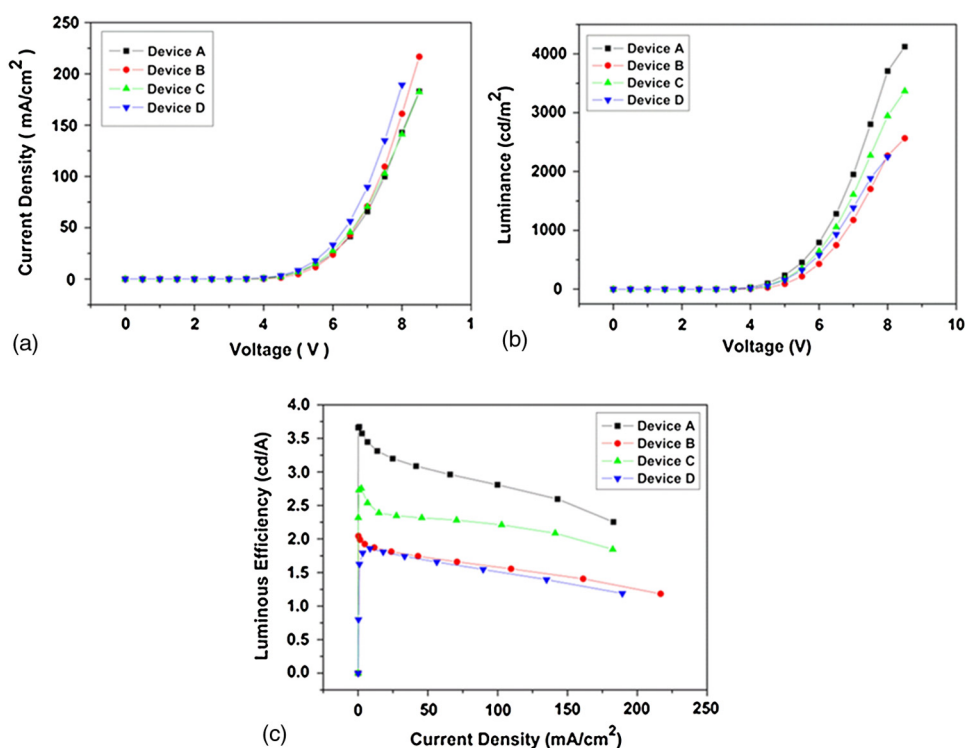


Fig. 2 The electrical and optical properties of devices A, B, C, and D; (a) current density–voltage, (b) luminance–voltage, and (c) luminous efficiency–current density.

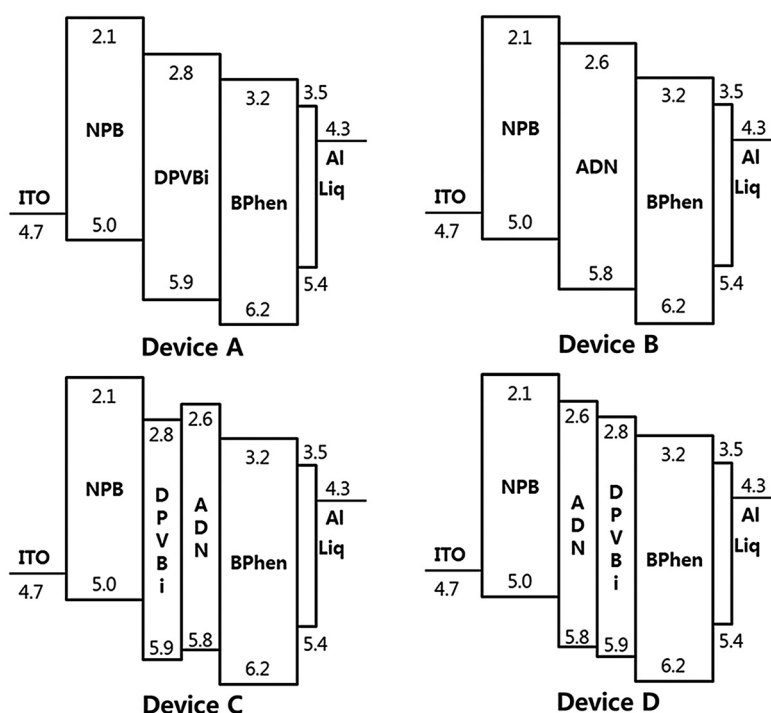


Fig. 3 Energy band diagrams of devices A to D.

respectively. Despite device D's structural advantage; an imbalance of electrons and holes is caused due to the fact that the ADN with ETL-like material is located next to the HTL. It results in lower luminance and luminous efficiency. In addition, DPVBi is a bipolar host material so that better carrier balancing is expected in the DPVBi. Devices A and C, in which DPVBi is placed next to the HTL, have higher luminance and luminous efficiency than the other two devices, although they have lower current density.

As can be seen from the device structures of devices A and C in Fig. 3 the large energy offset with adjacent layers acts as an effective barrier to block carrier flow through the electrodes. Both NPB and BPhen are used for electron and hole-blocking because of their higher HOMO and LUMO energy barriers against DPVBi of 0.7 and 0.5 eV, respectively. Therefore, electrons and holes are confined at the interface between the EML and the blocking layers, causing carrier balancing, as well as higher recombination probability, in the EML of DPVBi. Moreover, quantum wells are formed in device C to accumulate electrons and holes due to DPVBi's LUMO and ADN's HOMO energy levels. Since most of the recombination zone is generated at the interface of the EML and the HTL, holes and electrons are likely to be piled up and stocked at the quantum well, which results in higher luminance and luminous efficiency in device A.

Table 2 summarizes the CIE_{xy} coordinates of fabricated blue OLEDs with various voltages. All measured color coordinates of the devices indicate that they emit deep blue light and the color coordinates improve with increasing voltage. Device B generates the closest to a deep blue emission with CIE_{xy} coordinates of (0.157, 0.117) at 8 V.

As mentioned above, devices A and C show higher luminance and luminous efficiency compared to the other two devices. Then, we fabricated devices E and F having the same device

Table 2 CIE_{xy} color coordinates of devices A to D at voltages of 4, 6, and 8 V.

	Device A	Device B	Device C	Device D
4 V	(0.152, 0.204)	(0.161, 0.139)	(0.153, 0.160)	(0.162, 0.167)
6 V	(0.152, 0.201)	(0.159, 0.126)	(0.153, 0.155)	(0.158, 0.152)
8 V	(0.152, 0.198)	(0.157, 0.117)	(0.153, 0.151)	(0.157, 0.141)

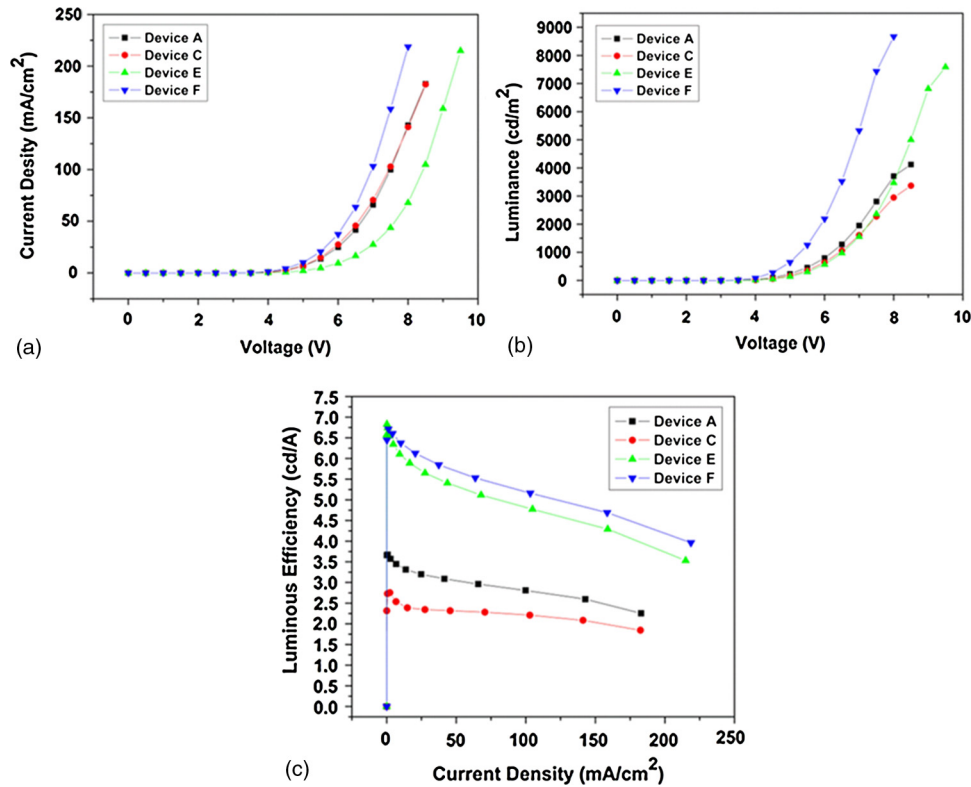


Fig. 4 The electrical and optical properties of devices A, C, E, and F; (a) current density–voltage, (b) luminance–voltage, and (c) luminous efficiency–current density.

structures as devices A and C, but using BCzVBi dopant in the EML to investigate the effect of the host–dopant system. The current density versus voltage curve of devices E and F are shown in Fig. 4. Even though devices A and C have similar current density to each other in the range of the applied voltage, it is found that device F has significantly higher current density than device E and the current density of device E is even lower than that of device A. Examining the energy band diagram of device E in Fig. 5, hole transport readily occurs from NPB to BCzVBi rather than DPVBi because the HOMO energy level of BCzVBi is 0.4 eV higher than that of DPVBi. On the other hand, electron transport is blocked by BCzVBi and is more likely to happen to DPVBi considering the LUMO energy level of DPVBi.

Plots of luminance versus bias voltages and the luminous efficiency versus current densities of devices E and F are shown in Fig. 4(b) and 4(c). The luminance and luminous efficiency of device E are 3472 cd/m² at 8 V and 4.77 cd/A at 104.82 mA/cm² and that of device F are 8668 cd/m² at 8 V and 5.16 cd/A at 103.20 mA/cm², respectively. Luminous efficiency of device F is similar to device E at low current density; however, when increasing current density,

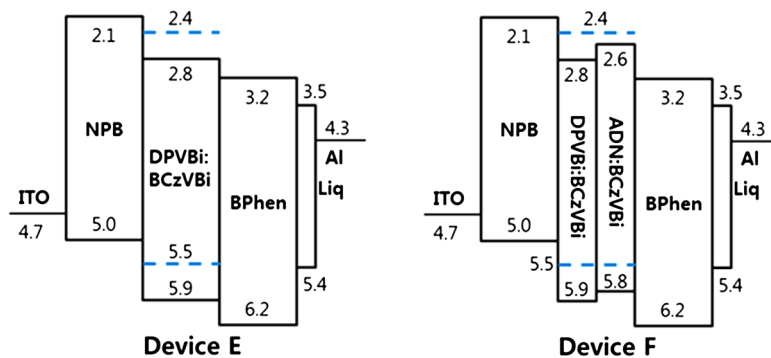


Fig. 5 Energy band diagrams of devices E and F using BCzVBi blue dopant.

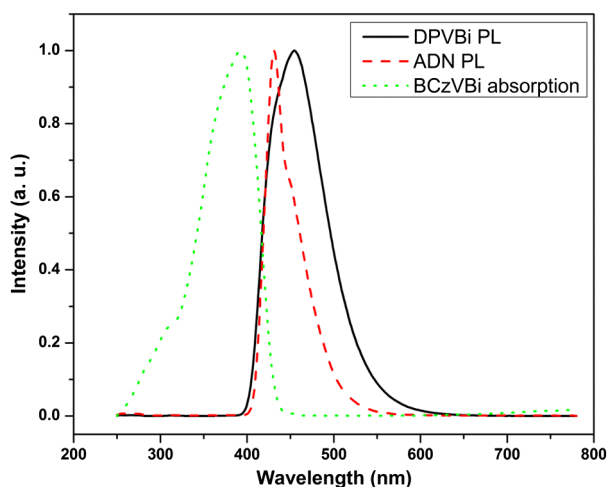


Fig. 6 The absorption of BCzVBi dopant and photoluminescence of ADN and DPVBi.

device F shows lower luminous efficiency roll-off compared to device E, because electrons are trapped at the surface of DPVBi and BPhen in device E due to the LUMO energy gap of 0.8 eV between BCzVBi and BPhen.

By doping fluorescent BCzVBi into the EML we achieved enhanced luminance in blue OLEDs compared to nondoped devices due to Förster energy transfer between host and dopant materials. Förster energy transfer is heavily dependent on the overlap of emission from host and absorption from dopant. Efficient Förster energy transfer will occur when the exciton energy from DPVBi host is transferred to BCzVBi dopant, as shown in Fig. 6.

Although device C has dual EMLs, it still has lower luminous efficiency than the single-layer device A. This is because holes and electrons are confined mainly in the DPVBi layer to lead to more effective exciton generation in device A. However, the doped dual-EMLs device F shows higher luminous efficiency than the doped single-layer device E. This result can be explained with an endothermic energy transfer between the host and dopant material. The endothermic energy transfer occurs in BCzVBi-doped devices because of the higher LUMO energy level of BCzVBi than that of DPVBi. The endothermic energy transfer between BCzVBi's LUMO and DPVBi's LUMO is facilitated due to thermal excitation of accumulated electrons in the LUMO of DPVBi and migration of holes in BCzVBi's HOMO from DPVBi's HOMO energy level. Furthermore, electrons in ADN not only move to the quantum well but also transfer energy to BCzVBi by endothermic energy transfer and this enhances luminous efficiency of device F.

The CIE_{xy} coordinates of devices E and F are (0.153, 0.252) and (0.153, 0.207) at 8 V, respectively. The color coordinates from devices E and F are far off from those of nondoped devices. The excitons from BCzVBi-doped EMLs are possibly emitted without enough energy for blue emission due to the energy level of the host and dopant material; that is, the excitons are trapped at the HOMO energy level of BCzVBi. In addition, the color coordinates of device F are relatively closer to deep blue emission than that of device E, because ADN has better color purity when inserted in the EML.

4 Conclusions

Blue OLED devices using single and dual EMLs were fabricated and their electrical and optical characteristics were compared. A host-dopant system was applied to improve luminous efficiency and color purity based on CIE_{xy} coordinates to optimize blue OLED performances. Among the blue OLEDs, device F with dual EMLs using BCzVBi as a fluorescent dopant in the host of ADN and DPVBi shows the highest current density, luminance, and luminous efficiency of 189.3 mA/cm², 8668 cd/m² at 8 V, and 5.16 cd/A at 103.20 mA/cm², respectively, whereas device B emits deep blue emission with CIE_{xy} coordinates at (0.157, 0.117) at 8 V. Förster and endothermic energy transfer between host and dopant materials enhanced the

device's efficiency. The quantum well structure between the EML, HTL, and ETL plays a role in improving exciton formation via effective carrier confinement to achieve better device properties.

Acknowledgments

These works have been financially supported by the Natural Sciences and Engineering Research Council of Canada under the Discovery Grants program and the Ministry of Knowledge Economy through the fostering project of the Industrial-Academic Cooperation Centered University in Korea.

References

1. A. R. Duggal et al., "Organic light-emitting devices for illumination-quality white light," *Appl. Phys. Lett.* **80**(19), 3470–3472 (2002), <http://dx.doi.org/10.1063/1.1478786>.
2. H. Kanno, Y. Hamada, and H. Takahashi, "Development of OLED with high stability and luminance efficiency by co-doping methods for full color displays," *IEEE J. Sel. Topics Quantum Electron.* **10**(1), 30–36 (2004), <http://dx.doi.org/10.1109/JSTQE.2004.824076>.
3. J. Kido, M. Kimura, and K. Nagai, "Multilayer white light-emitting organic electroluminescent device," *Science* **267**(5202), 1332–1334 (1995), <http://dx.doi.org/10.1126/science.267.5202.1332>.
4. C. W. Tang and S. A. VanSlyke, "Organic electroluminescent diodes," *Appl. Phys. Lett.* **51**(12), 913–915 (1987), <http://dx.doi.org/10.1063/1.98799>.
5. Y. Kijima, N. Asai, and S. Tamura, "A blue organic light emitting diode," *Jpn. J. Appl. Phys. Part 1* **38**(9A), 5274–5277 (1999), <http://dx.doi.org/10.1143/JJAP.38.5274>.
6. Y. Kan et al., "Highly-efficient blue electroluminescence based on two emitter isomers," *Appl. Phys. Lett.* **84**(9), 1513–1515 (2004), <http://dx.doi.org/10.1063/1.1651653>.
7. T. C. Chao et al., "Highly efficient UV organic light-emitting devices based on bi(9,9-diarylfluorene)s," *Adv. Mater.* **17**(8), 992–996 (2005), [http://dx.doi.org/10.1002/\(ISSN\)1521-4095](http://dx.doi.org/10.1002/(ISSN)1521-4095).
8. S. Tao et al., "Highly efficient non-doped blue organic light-emitting diodes based on fluorene derivatives with high thermal stability," *Adv. Funct. Mater.* **15**(10), 1716–1721 (2005), [http://dx.doi.org/10.1002/\(ISSN\)1616-3028](http://dx.doi.org/10.1002/(ISSN)1616-3028).
9. Y. Divayana et al., "Efficient blue organic light-emitting device based on N, N'-di(naphth-2-yl)-N, N'-diphenyl-benzidine with an exciton-confining structure," *Appl. Phys. Lett.* **89**(17), 173511 (2006), <http://dx.doi.org/10.1063/1.2364161>.
10. M. T. Lee et al., "Stable styrylamine-doped blue organic electroluminescent device based on 2-methyl-9,10-di(2-naphthyl) anthracene," *Chem. Appl. Phys. Lett.* **85**(15), 3301–3303 (2004), <http://dx.doi.org/10.1063/1.1804232>.
11. M. H. Ho et al., "Highly efficient deep blue organic electroluminescent device based on 1-methyl-9,10-di(1-naphthyl) anthracene," *Appl. Phys. Lett.* **89**(25), 252903 (2006), <http://dx.doi.org/10.1063/1.2409367>.
12. R. Baer and E. Rabani, "Theory of resonance energy transfer involving nanocrystals: the role of high multipoles," *J. Chem. Phys.* **128**(18), 184710 (2008), <http://dx.doi.org/10.1063/1.2913247>.
13. J. R. Lakowicz, *Principles of Fluorescence Spectroscopy*, Springer, New York (2006).
14. Y. Hamada et al., "Red organic light-emitting diodes using an emitting assist dopant," *Appl. Phys. Lett.* **75**(12), 1682–1684 (1999), <http://dx.doi.org/10.1063/1.124790>.
15. C. W. Tang, S. A. Van Slyke, and C. H. Chen, "Electroluminescence of doped organic thin films," *J. Appl. Phys.* **65**(9), 3610–3616 (1989), <http://dx.doi.org/10.1063/1.343409>.
16. A. A. Shoustikov, Y. Yujian, and M. E. Thompson, "Electroluminescence color tuning by dye doping in organic light-emitting diodes," *IEEE J. Sel. Topics Quantum Electron.* **4**(1), 3–13 (1998), <http://dx.doi.org/10.1109/2944.669454>.
17. S. E. Shaheen et al., "Energy and charge transfer in organic light-emitting diodes: a soluble quinacridone study," *J. Appl. Phys.* **85**(11), 7939–7945 (1999), <http://dx.doi.org/10.1063/1.370612>.

18. K. M. Vaeth and C. W. Tang, "Light-emitting diodes based on phosphorescent guest/polymeric host systems," *J. Appl. Phys.* **92**(7) 3447–3453 (2002), <http://dx.doi.org/10.1063/1.1501748>.
19. Y. Kawamura, S. Yanagida, and S. R. Forrest, "Energy transfer in polymer electrophosphorescent light emitting devices with single and multiple doped luminescent layers," *J. Appl. Phys.* **92**(1), 87–93 (2002), <http://dx.doi.org/10.1063/1.1479751>.
20. F. C. Chen et al., "Energy transfer and triplet exciton confinement in polymeric electrophosphorescent devices," *J. Polymer Sci. Part B.* **41**(21), 2681–2690 (2003), [http://dx.doi.org/10.1002/\(ISSN\)1099-0488](http://dx.doi.org/10.1002/(ISSN)1099-0488).
21. C. C. Wu, J. C. Sturm, and A. Khan, "Surface modification of indium tin oxide by plasma treatment: an effective method to improve the efficiency, brightness, and reliability of organic light emitting devices," *Appl. Phys. Lett.* **70**(11), 1348–1350 (1997), <http://dx.doi.org/10.1063/1.118575>.
22. S. Y. Oh et al., "Characteristics and fabrication of polymer light emitting diode using copolymer having perylene and triazine moieties in the polymer side chain," *J. Ind. Eng. Chem.* **12**(1), 69–75 (2006).
23. Y. H. Ho et al., "High-efficiency and long-lifetime fluorescent blue organic-emitting device," *Proc. SPIE* **6333**, 633303 (2006), <http://dx.doi.org/10.1117/12.678220>.

Biographies and photographs of the authors not available.